Instrument Science Report COS 2020-07

Cycle 26 COS FUV Detector Gain Maps

David Sahnow[1]

[1]*Space Telescope Science Institute, Baltimore, MD*

30 September, 2020

ABSTRACT

Program 15534 used the onboard deuterium lamp to illuminate the regions of the COS FUV detector used during normal operations in Cycle 26. Data were taken two times during the year at detector positions corresponding to Lifetime Position 2 (LP2), LP3, and LP4. The pulse height information obtained was used to create gain maps in order to monitor the detector gain sag. The results obtained are consistent with those from previous cycles.

Contents

1. Introduction

Monitoring the gain (the number of electrons generated by the microchannel plate stack for each incident photon) of the COS FUV detector is crucial to ensure optimal performance. When the modal gain (the peak of the pulse height distribution; see Clampin 1997, Figure 6) at a particular location on the detector drops below a value of about 3, approximately 5% of the counts there fall below the lower pulse height threshold, which leads to an apparent local loss of sensitivity (Sahnow et al. 2011). The amount of gain sag is a function of the number of photon events incident on the detector, the high voltage (HV), and other factors. The largest gain drops are seen in the regions of the detector where Lyman-α airglow lines fall, since they have collected the most counts.

Gain map files are created at each commanded HV approximately weekly by measuring the modal gain from Pulse Height Distributions (PHDs) made using all of the counts collected during the TIME-TAG science exposures that have executed during that time. However, since ~25 counts in a binned pixel are necessary to reliably measure the peak of the PHD, the regions of the detector where the gain can be measured varies from week to week, depending on the data taken. For areas on the wings of the cross dispersion profiles, it may be rare to ever collect enough counts for a valid measurement in any one week period.

In order to ensure more complete areal coverage at each Lifetime Position (LP) and HV, exposures of the internal deuterium lamp are also occasionally obtained. These lamps illuminate a wider area in the cross-dispersion direction (y axis) of the detector so that modal gain measurements can be made everywhere that photons from science targets fall. These gain map exposures are taken both before and after any change to the nominal detector high voltage or Lifetime Position, and at approximately six month intervals when the voltage is not changed. Because of the strongly varying intensity of the lamp as a function of wavelength, data is collected using both G130M/1309 and G160M/1600. The former is the best choice for obtaining approximately uniform coverage on Segment A, while the latter does the same for Segment B. In order to maximize the number of counts in the PHD, data from both central wavelenths is combined when creating the gain maps.

2. Execution

During Cycle 26, Program 15534 obtained deuterium data during eight one-orbit visits, which are listed in Table 1; all visits successfully collected the expected data. Each visit followed the same procedure:

- Adjust the HV values to the appropriate levels
- Adjust the aperture block in the cross-dispersion direction so that the deuterium lamp illuminates the appropriate region on Segment A when using G130M/1309
- Take a 400 second deuterium lamp exposure at FP-POS=1 using both detector segments
- Adjust the aperture to a second cross-dispersion location to obtain additional coverage on Segment A and take a 400 second deuterium lamp exposure at FP-POS=4 using both detector segments

- Adjust the aperture in the cross-dispersion direction so that the deuterium lamp will illuminate the appropriate region on Segment B when using G160M/1600
- Take a 400 second deuterium lamp exposure using both detector segments
- Adjust the aperture to a second cross-dispersion location to obtain additional coverage on Segment B and take another 400 second deuterium lamp exposure
- Return the aperture to the nominal LP4 location
- Return the HV to the nominal values for the standard observing modes

The two offset positions for each grating were chosen so that when the data from the exposures are combined, the count rate is roughly uniform in the cross-dispersion direction and they overlap with the science spectra at the same LP. The aperture offset values used (LAPXSTP) are shown in Table 1; these were determined by measuring the position of spectra as a function of aperture position during previous deuterium lamp observations. In several cases, the calculated value of LAPXSTP would have moved the aperture block beyond its soft stop at -275. In those cases, a value of -267 was used.

The visits were labeled such that the first character denoted the Lifetime Position (2 for LP2, etc.). The second character in the visit label was A for the first visit at that LP in the spring, and C for the first visit in the fall. For LP4, where multiple HV values were used in each case, B was used for the second visit in the spring, and D for the fall.

Visit 2A executed at LP2 on April 1, 2019 to obtain a lamp spectrum at LP2, using the Blue Modes HV values of 173/175 for Segment A/B.

Visit 3A obtained spectra at LP3 on April 1, 2019. It used the HV values of 167/175 appropriate for standard mode spectra taken at LP3.

Visits 4A and 4B executed at LP4 on April 1, 2019. They used HVs appropriate for the standard modes (163/163; 4A) and G130M/1222 (163/167; 4B).

Visits 2C, 3C, 4C, and 4D all ran on October 1, 2019; positions and voltages matched those of the corresponding April visits.

Additional contingency visits would have been used to obtain data immediately before and after any change in the nominal HV values during the cycle, but these were not needed since no HV changes were made.

Table 1. Visits executed in Program 15534

Root Name	Vis	Date	LP	Mode	HV (A/B)	LAPXSTP (G130M)	LAPXSTP (G160M)
ldv62a*	2A	4/1/19	2	Blue	173/175	-213,-267*	-225,-267*
ldv63a*	3A	4/1/19	3	Standard	167/175	-72,-128	-84,-140
ldv64a*	4A	4/1/19	4	Standard	163/163	-32,-86	-41,-95
ldv64b*	4B	4/1/19	4	1222	163/167	-32,-86	-41,-95
ldv62c*	2C	10/1/19	2	Blue	173/175	-213,-267*	-225,-267*
ldv63c*	3C	10/1/19	3	Standard	167/175	-72,-128	-84,-140
ldv64c*	4C	10/1/19	4	Standard	163/163	-32,-86	-41,-95
ldv64d*	4D	10/1/19	4	1222	163/167	-32,-86	-41,-95

* The commanded value of LAPXSTP for these position set to -267 in order to avoid the soft stop at -275

3. Summary of Analysis and Results

The standard gain map creation routines were used to calculate the modal gain; they fit a gaussian to the pulse height distribution for each binned pixel, and the value of the peak of that fit is taken as the modal gain. Figure 1 shows the modal gain as a function of X pixel near the center of the LP4 detector location for both the April and October visits, along with the data obtained in October 2018 as part of Program 14941. Figure 2 shows an expanded view around the regions with the most counts for each segment. The Segment B figure shows that the drop in modal gain is much stronger at the two x positions where Lyman-α falls at LP4. Note that these figures show the gain at a constant Y pixel across the detector; the Y value was chosen to pass through the regions of lowest gain, but doesn't necessarily show the lowest value at each X position.

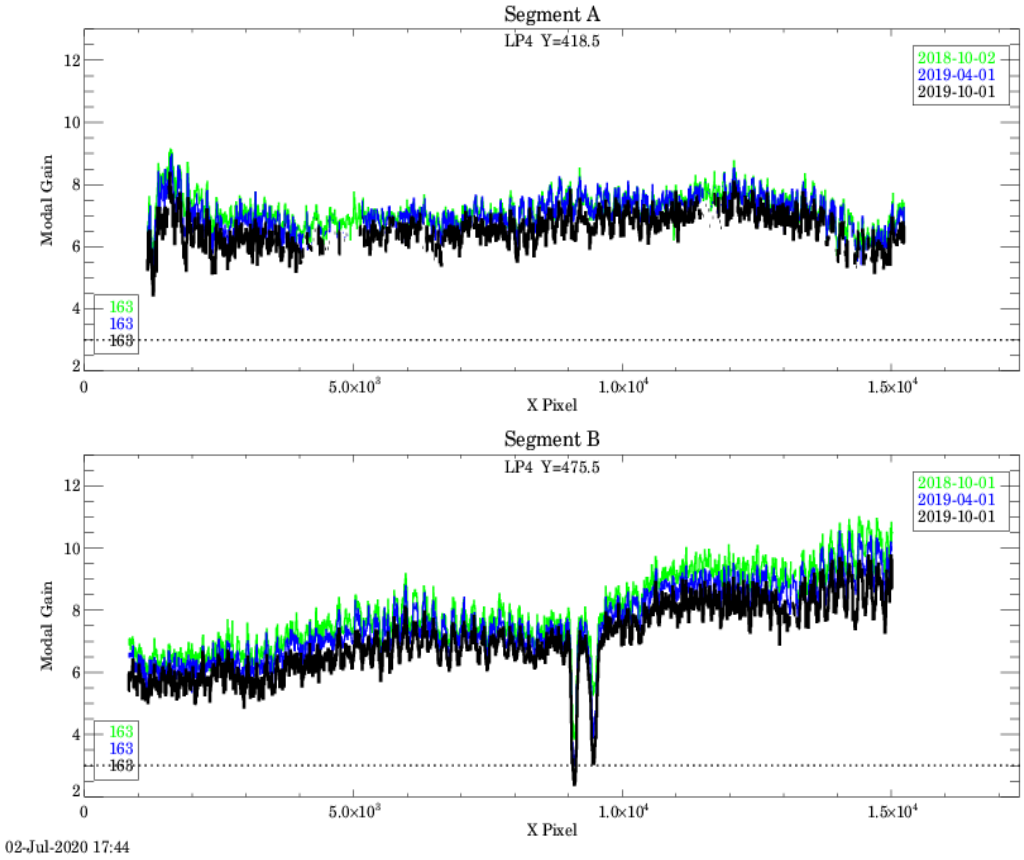

Figure 1. Modal gain as a function of X pixel at the center of the LP4 region of the detector at the end of Cycle 25 from Program 14941 (**green**) and at two times during Cycle 26 from Program 15534 (**blue** and **black**). As expected, there is a decrease in the overall gain as a function of time, with a variation as a function of position due to varying exposure levels. A much larger decrease in modal gain is seen at the positions of the Lyman-α lines near pixel 9000 on Segment B (see Figure 2). The gap in the 2019 measurements at several locations on Segment A is due to having too few counts to make a reliable measurement; the counts will be increased in the Cycle 27 program.

The modal gain measured at LP3 at the same times as in the previous figures is displayed in Figure 3, and Figure 4 shows an expanded view highlighting the deepest gain sag holes on each segment. In this case, the holes have dropped to a modal gain of 3 or below on Segment B, which is operating at the maximum allowable HV value of 175. On Segment A, the gain remains above 3 everywhere, and the HV has not yet been raised to its maximum allowed value.

Figure 5 shows the modal gain at the center of the LP2 region for the same times as the other LPs. Very little change has occurred during Cycle 26 since the number of counts that fell on this region of the detector is much smaller than at LP3 or LP4.

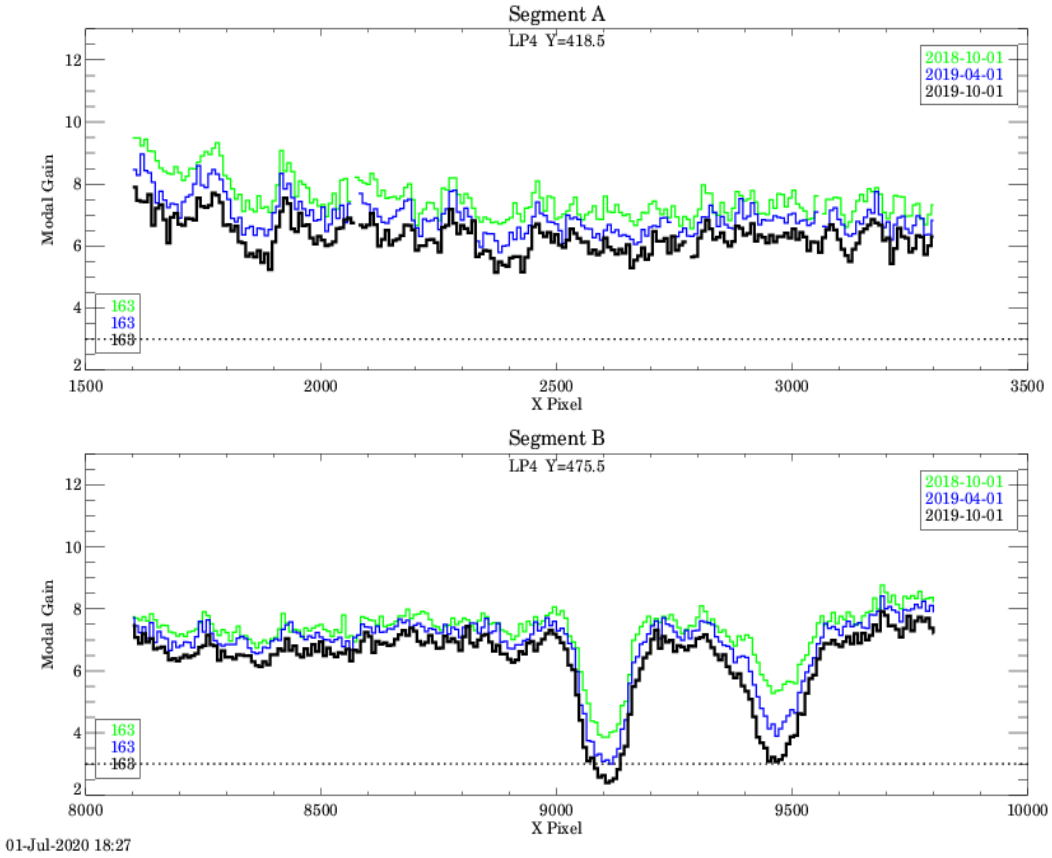

Figure 2. Zoomed in view of the data shown in Figure 1. This view highlights the significant drop in modal gain on Segment B at the positions corresponding to the Lyman-α lines from G130M/1291, FP-POS 3 and 4. These are the only FP-POS values that place Lyman-α on this segment at LP4. We allow the modal gain at these locations to drop below 3.

The primary purpose of this program was to obtain gain maps which are used to determine the slope of the modal gain vs. extracted charge curve over the entire illuminated area of the detector at all of the nominal high voltage values used during the cycle. Making regular measurements allows a more accurate determination of these slopes, which leads to more accurate predictions of when the gain is likely to drop to 3, and thus when a high voltage change or Lifetime Position change is needed. Examples of gain vs. extracted charge curves are shown in Sahnow et al. (2011).

Data from this program, along with data from other gain measurements, is also used in the construction of the gain sag reference table (GSAGTAB), which flags the regions where the modal gain has dropped too low.

The results described above are consistent with those from previous cycles, e.g. Sahnow (2019) for Cycle 25. Regular gain map measurements will continue in Cycle 27 as Program 15711.

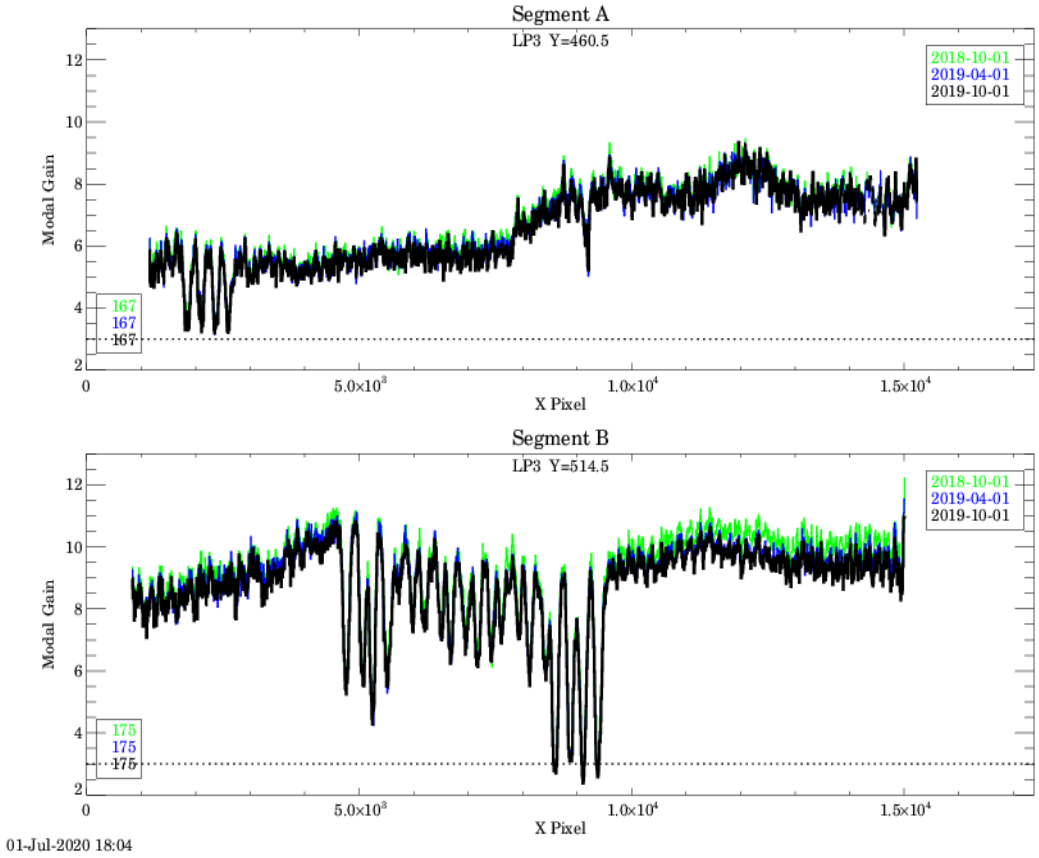

Figure 3. Modal gain as a function of X pixel at the center of the LP3 region of the detector using the LP3 G130M/1222 HV values of 167/175.

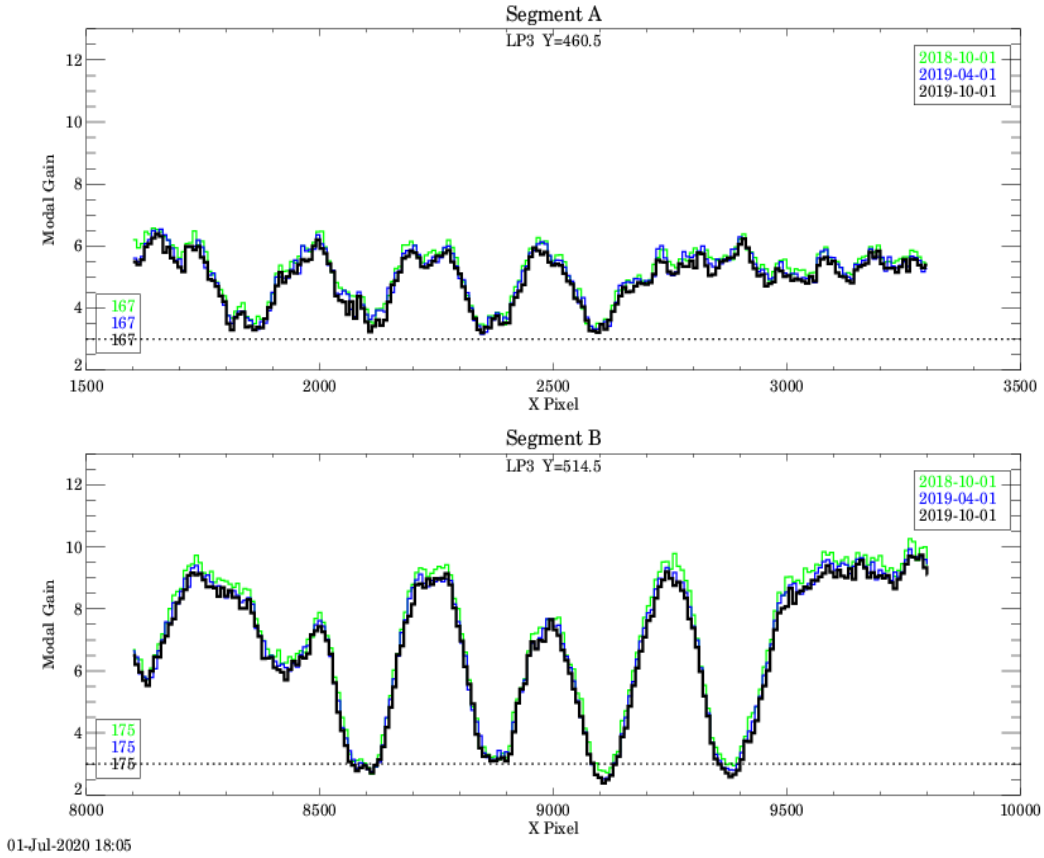

Figure 4. An expanded view of a portion of the modal gain plot shown in Figure 3. All four Lyman-α lines due to G130M/1291 at LP3 on Segment B have dropped to a modal gain of ~3 at HV=175. On Segment A, the four Lyman-α impacted regions are approaching this value, but since the current HV is only 167, it can be raised before a loss of counts occurs.

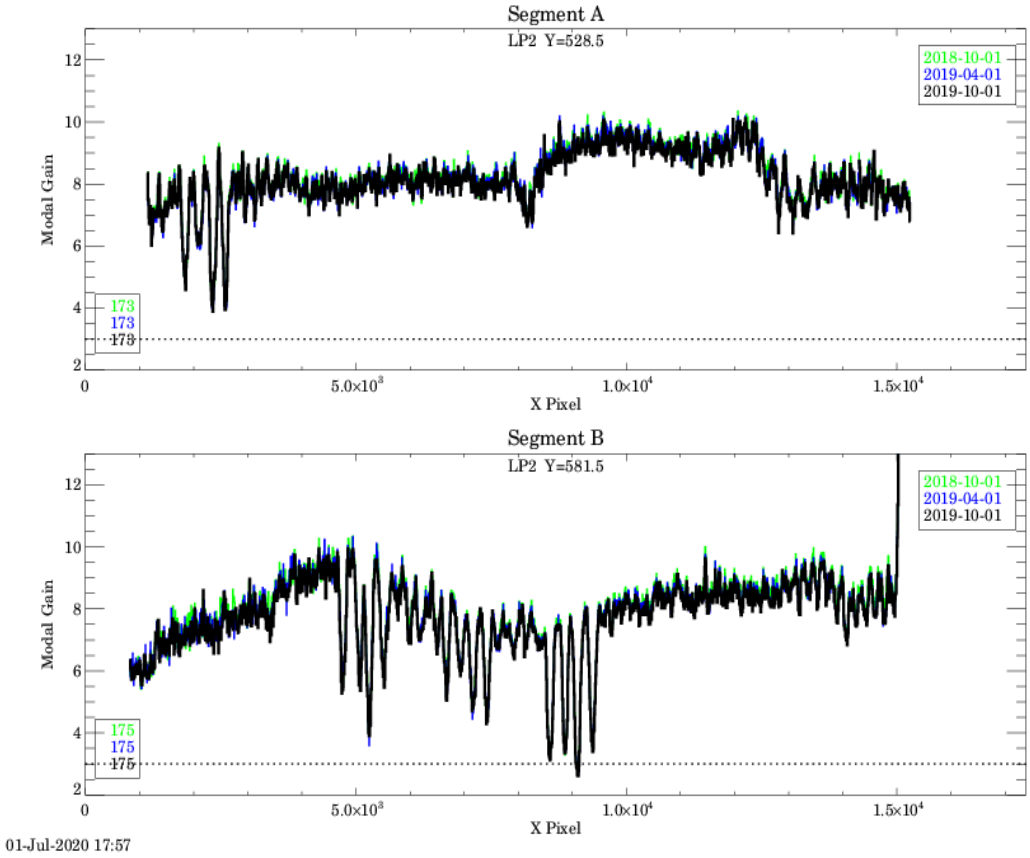

Figure 5. Modal gain as a function of X pixel at the center of the LP2 (Blue Mode) region of the detector using the Blue Modes HV values of 173/175. There was very little change during this cycle, which is not surprising since this mode is not used extensively. The deepest hole has a modal gain of ~3, where throughput losses are ~5%.

Change History for COS ISR 2020-07

Version 1: 30 September 2020

References

Clampin, M. 1997, STIS ISR 96-31, "Bright Object Protection Mechanisms for STIS"

Sahnow, D., et al. 2011, "Gain sag in the FUV detector of the Cosmic Origins Spectrograph", Proc. SPIE 8145, 8145Q

Sahnow, D. 2019, COS ISR 2019-21, "Cycle 25 COS FUV Detector Gain Maps"